3D Vision Sensing Technologies in Factory Automation and Robotics

Mattias Johannesson
SICK IVP, Wallenbergs gata 4, 583 35 Linköping, Sweden
e-mail: mattias.johannesson@sick.com

Abstract

The topic of this paper is 3D Machine Vision Applications in Factory Automation and Robotics seen in the perspective of the development of CMOS imaging technology and the possibilities this has given SICK to realize technology and market leading 3D vision systems.

First we discuss the sensor-processor design. The integration of processing and sensing on the same CMOS sensor chip gives powerful, fast and compact systems. We then describe the current M12 sensor and how it is used to implement efficient 3D algorithms using laser triangulation. We also compare this technology with other 3D imaging technologies and give details on two successful application areas for our cameras.

1. CMOS Imaging History

The history of CMOS imaging for machine vision started in earnest in the early nineties. At this point only solid-state CCD technology was widely available. The CCD technology required fabrication in special processes, device control required complicated analog controls and external AD conversion was needed. CMOS technology on the other hand promised fabrication of image sensors in standard CMOS processes, and the combination of analog sensor circuitry and digital logic made it possible to integrate AD conversion and other digital circuits on the same die. Overviews of the state of the art in the mid-nineties from the CMOS sensor pioneer Eric Fossum are given in [23][24]. Today almost twenty years later CMOS imaging technology has surpassed CCD for most applications and analog film is more or less dead as a media.

1.1. IVP sensor history

IVP, Integrated Vision Products, was started 1985 by researchers at Linköping University with the idea to combine processing and sensing on the same CMOS chip. The idea had been presented and patented by the company founders 1983 [17][25]. In 1987 the first product LAPP1100 was launched. This combined a linear array of 128 photo-diodes with a linear array of 128 bit-serial processors. The sensor did not have a traditional AD-converter, but the processors together with the possibility to poll the photo-diodes in a non-destructive way nevertheless made it possible to implement advanced grayscale image processing. The architecture then lead to the development of the Near-Sensor Image Processing, NSIP, paradigm where a binary signal studied over time can give very high dynamic range handling [20][21]. The sensor was implemented in a 3 μm process with 50 micron pixel size.

In the early 1990's the MAPP2200 sensor incorporated extensions to the processor, programmable AD-converters and 256x256 pixels [18][19]. The sensor had 32 micron pixels and was implemented in a 1.6 micron process. Even with the introduction of the AD-converter the non-destructive NSIP-compatible readout technology was kept, and this device was used in research on sheet-of-light range imaging, starting with practical investigations on the ideas for an application specific NSIP-based imager with processing in each pixel [1][2][20]. The research using the MAPP2200 sensor for range imaging expanded into algorithms using conventional non-NSIP-based algorithms, and these proved to work well on this device [1][3][4].

The research was incorporated into the product offer IVP RANGER 1994, where the MAPP2200 camera was sold with the sheet-of-light triangulation software.

Several generations of sensors and camera systems have been developed and deployed leading up to the current M12 sensor based systems.

1.2. The M12 sensor

The M12 sensor has 1536x512 pixels is implemented in a 0.35 micron CMOS process, and has 9.5 micron pixel pitch. The chip runs on a 33 MHz clock and has an IO bandwidth of 1 Gbit/s through a 32-bit interface. Control is through a 24-bit instruction.

The M12 sensor has been in production since 2002, and is currently used in the Ranger, Ruler and IVC-3D product families from SICK who bought IVP 2003. A more detailed overview of the sensor is found in [22]. A functional block diagram seen in Figure 1, and a photo in Figure 2.

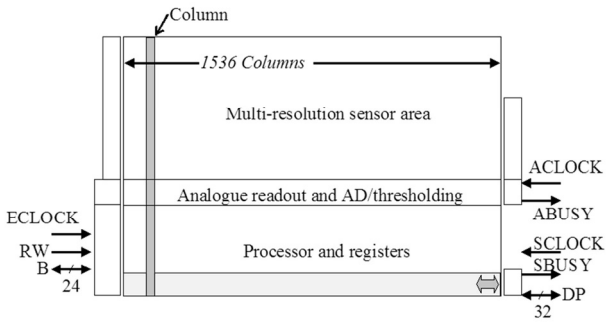

Figure 1. M12 Chip block diagram with IOs and control indicated.

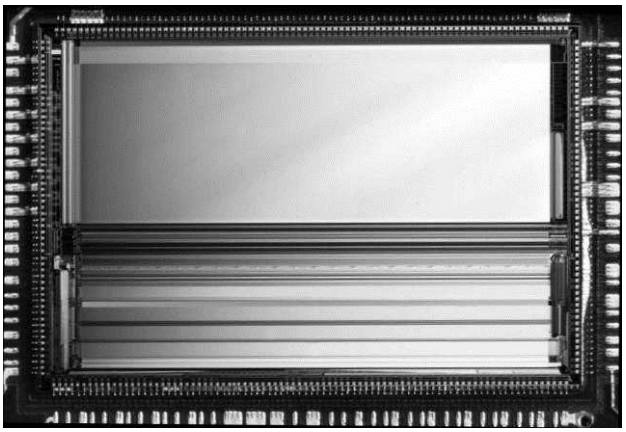

Figure 2. An image of the M12 die. The top part is the sensor area. The processors and IO registers are at the bottom.

1.3. Image Sensor

M12 is the first sensor in the MAPP family using active pixels. A feature of the older MAPP designs, and typical of passive pixels, was the extensive use of analog binning. This was a key to extract weak laser scatter signals, and therefore pixel binning capability was kept even with the active pixel design.

The pixels are of the 3-transistor rolling-shutter design. Non-correlated double sampling is used to reduce fixed pattern noise, and the image quality is very good with a global FPN of < 1% RMS. Since the raw pixel data typically is processed directly on the sensor there is no possibility to correct large fixed pattern noise, so the low FPN is a critical feature.

The AD converters are programmable ramp AD converters capable of 4 to 8 bit conversions. The analog readout stage contains a selectable amplification so that a gain of 1, 3 or 4 can be selected. The pixel and readout circuitry is shown in Figure 3.

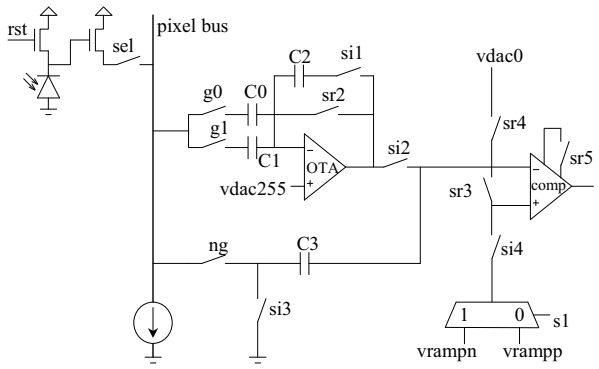

Figure 3. The pixel and readout circuit design. C0 and C1 have different size and are used for the gain control.

A new feature in this sensor is the high-resolution extension to the array [28]. This extension contains a small number of sensor rows with a pitch of 4.75 microns, giving 3072 columns in the same space as the 1536 columns of the main part of the array. This extension gives gray scale line sensing with double resolution compared with the extracted 3D data.

The sensor was augmented with a line RGB filter option in 2010. The filters use a sharp band-pass design and an additional IR-blocking filter to avoid second order pass bands to transmit IR through the blue and green channels, see Figure 4. There is a set of RGB filters on the top rows of the main sensor array giving 1536 columns wide color data and an additional set on the high resolution part giving 3072 columns wide color data.

To further aid multi scan applications, where a strong white illumination is used for gray-scale/color imaging and a laser for ranging and laser scatter measurements a further IR filter option is available. This adds an IR-pass (visible blocking) filter to a large part of the main array. This makes this region suitable for use with IR lasers, giving little cross talk from a white LED-based light with low IR content used for gray scale and color imaging. See also Figure 13.

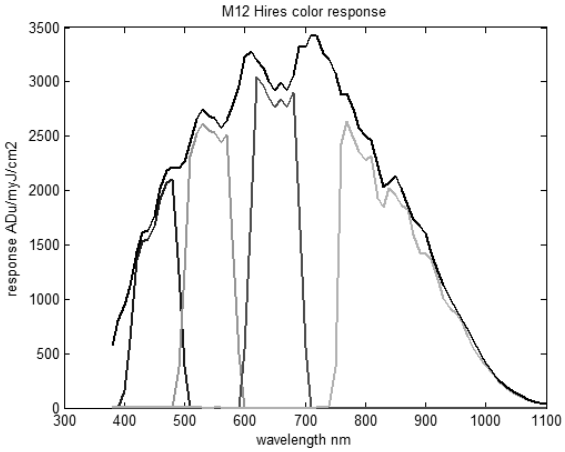

Figure 4. M12 sensor response as a function of light wavelength, and the transmission bands for the Blue, Green, Red and IR pass filters.

2. Processor

The processing array on the sensor is an extension on the design found in the older LAPP and MAPP sensors [17][18][19][20]. An overview of the processor and pixel column is seen in Figure 5.

The IO registers contain 16 bits, and 2 neighboring columns are output every clock cycle through a 32-bit interface. At the 33 MHz clock this gives 1 Gbit/s. The main processing is made using the PLU – Point Logic Unit. Typical *b*-bit arithmetical operations such as add requires *b-3b* clock cycles. The peak performance for 8-bit addition operations is in the order of 6 GOps/s.

The processor also contains an NLU allowing operations directly on data from the closest left and right-most neighbor processor, as well as the GLU implementing ripple-logic across the whole array. The GLU can for instance be used to make create an RL-coded version of a binary image very efficient [20].

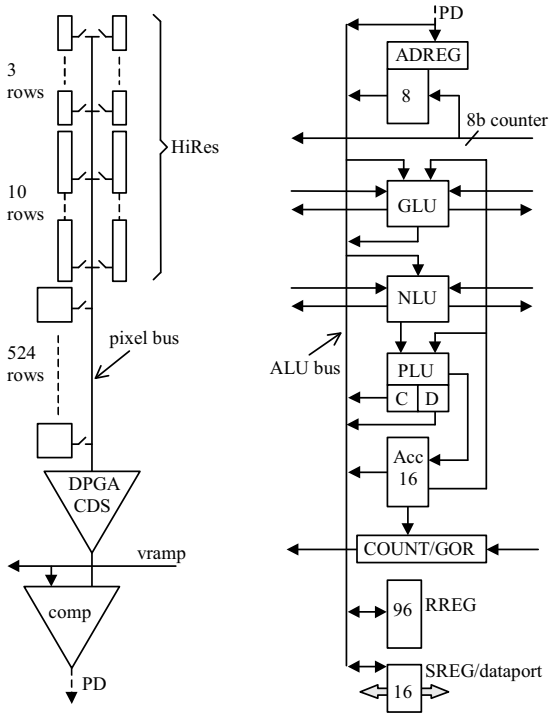

Figure 5. Column architecture of the sensor (left) and processor (right).

3. Sheet-of-Light triangulation

Range measurements using triangulation is a very old technology. It was known in the antique and was used in the measurements of the whole North-South length of France conducted to define the meter standard in the late eighteenth century in France [15].

One of the pioneering groups in research developing fast laser based triangulation systems was at NRC in Canada in the eighties [5]. These were based on a single linear array and clever scanning of a single point laser. Early sensor designs for fast sheet-of-light triangulation involved using an array of linear PSD devices [6][7].

3.1. Working principle

Typical setups for laser-based triangulation are seen in Figure 6. A camera and a laser are pointed towards the target from different locations, giving a triangulation baseline. The impact position of the reflected laser light on the sensor gives the range.

The height resolution close to the optical axis of the camera can be approximated as

$$\Delta Z \sim \frac{\Delta X}{\sin(\alpha)}$$

where ΔX is the pixel resolution across the line and ΔZ the pixel resolution in height. Typical angles are from around 15 to 50 degrees. A large angle gives better height resolution, but will also give more occlusion, where the camera cannot see the laser when it is hidden behind an object. An alternative also shown in the figure is to have a vertical camera and a tilted laser, which gives the following approximate Z resolution

$$\Delta Z \sim \frac{\Delta X}{\tan(\beta)}$$

A benefit of a vertically aligned camera is that with a large β angle the height resolution is very good. It also makes it easy to use the camera for standard 2D image processing in the same setup.

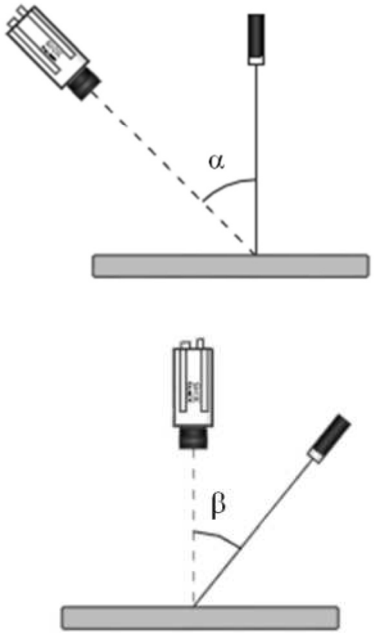

Figure 6. An illustration of a triangulation system using vertical laser (top) and vertical camera (bottom).

3.2. Processing

The key processing task in sheet-of-light triangulation is to extract the laser profile position in each sensor image, see Figure 7. This gives a very large data reduction from MxN pixels to N position values. The M12 sensor implements many different algorithms to extract the peak position. The fastest methods are based on thresholding the image and finding the start and end position of the peak in each column.

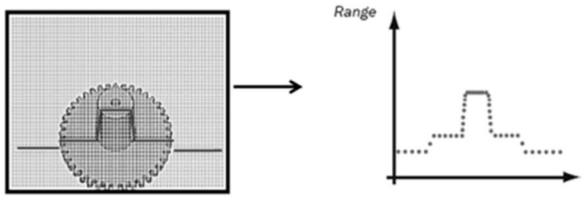

Figure 7. Illustration of the processing of one frame to obtain one 3D profile.

In the threshold algorithm the peak position is found using the average of a counter for the start and a counter for the end of the first peak seen in each column. The peak position counters are implemented using Gray code so that an increment can be implemented by inversion of a single bit. The start and end position indicators are temperature coded and kept in PLU registers C & D. The

inversion (increment) of the counters is then conditionally made using the C & D registers as second operands in an XOR operation. The instruction sequence for a program to find the start and end of a binarized peak is in pseudo code for a single row

```
FLAGCD PD          // Update C & D
XORC Acc(i)        // Count start pos
XORD Acc(j)        // Count end pos
```

and a visual representation is given in Figure 8. As long as the C and D register contents are 1 the counters increment, and after processing all rows the counter results are converted to standard binary code and summed together for a ½-pixel resolution average peak position.

Using this we reach close to 5 KHz profile extraction rate using all 512 rows of the sensor and can in the current camera system run up to 35 KHz profile rate using a smaller ROI. At 35 KHz the sustained throughput is around 3.5 G pixel/s and 430 Mbit/s output data.

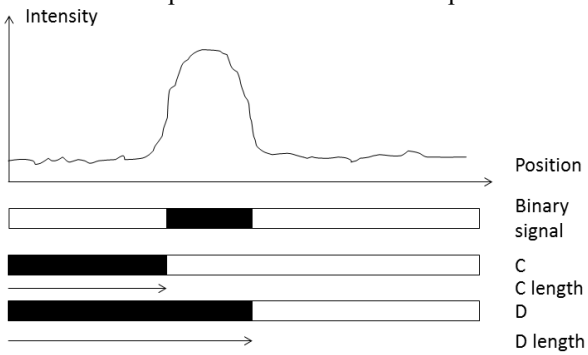

Figure 8. Illustration of the signals in binary peak position extraction. The peak mid position is given by the average of the C and D length counters.

Utilizing the AD converters the sensor implements a family of algorithms operating on grayscale data called Hi3D giving $1/16^{th}$ of a pixel in resolution. One example of a Hi3D algorithm is center-of-gravity which can be implemented very efficiently using iterative moment calculations [4][20].

For a center-of-gravity algorithm the inner loop for row x is

$$Sum(x) = Sum(x-1) + f(x)$$
$$XSum(x) = XSum(x-1) + Sum(x)$$

Typical bit resolution is 13 and 19 bits respectively, giving around 3*13+ 2*19 = 77 clock cycles, or around 2.5 micro seconds per row.

After processing all rows the position is given by the quotient of XSum and Sum

$$Cog = \frac{Xsum}{Sum} = \frac{\sum x * f(x)}{\sum f(x)}$$

The final division is not made inside the sensor; this has to be done in the camera or by the PC. Nevertheless a 2D region of rows is reduced on the sensor to 2 vectors representing the intensity (sum) and peak position for each column.

With Hi3D algorithms operating on 6-bit AD converter resolution we can reach above 3 KHz profile rate for a 128 row FOV, and around 1 KHz for the full sensor.

3.3. Multi Scan

A key feature of the Mapp sensor family is the ability to acquire several different measurements simultaneously. This is done using the complete random access of the sensor and the programmability of the processor [16].

From the triangulation laser we normally get position and intensity. The intensity from the laser is however not as good as intensity from a non-coherent light source and we can assign a region of the sensor to use for grayscale imaging. There are also optional color filters covering a few sensor rows, so that the camera can be used as a line scan color camera in addition to the 3D imaging.

A further multi-scan measurement is that of laser scatter [16][26]. Here the amount of light detected *beside* the main reflected light tells about the internal structure of the material – how much light is transported through the material to exit at a different position than the entry point. The most common application for this is in wood, where healthy wood fibers transmit light 1-2 mm away from the light entry. Grain "diving" into the wood in a knot, or areas affected by rot does not show this "halo" effect. An illustration of a sensor image with three outlined multi scan regions is shown in Figure 9, and a result image in Figure 10.

We also have algorithms for Hi3D calculations who in addition to high precision peak position and peak intensity also delivers a measure of the laser scatter, used for instance in wood inspection as described below [27][29].

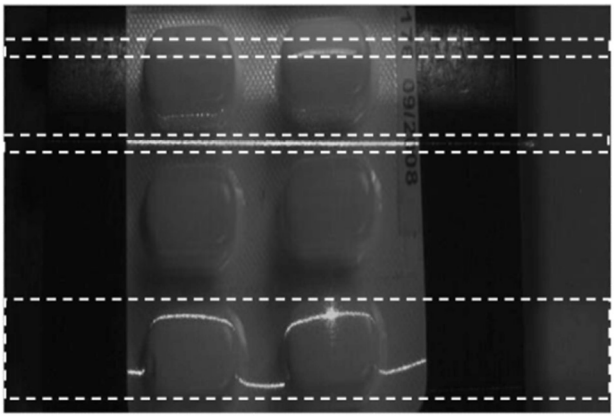

Figure 9. A sensor image with a region for 3D (bottom), a region for laser scatter (mid) and a region for grayscale (top) are shown.

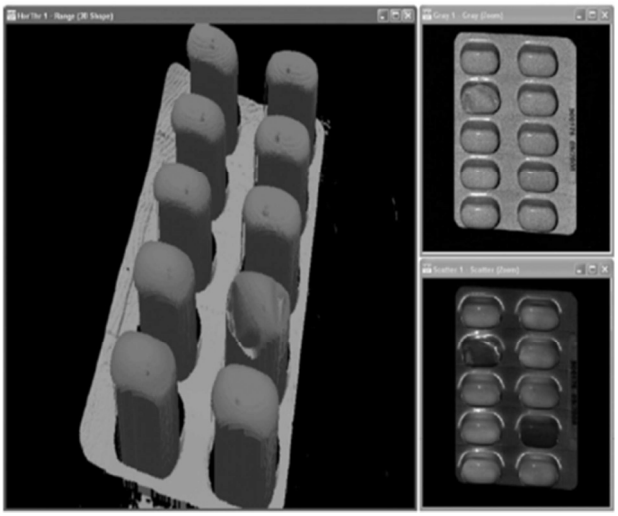

Figure 10. An example of a blister pack with rendered 3D (left), grayscale (top) and laser scatter (bottom). The scatter image clearly shows 2 empty blisters.

3.4. Sheet-of-light triangulation features

The sheet-of-light triangulation technology is fast and robust. It can be scaled between systems with a few microns in resolution to larger systems with field-of-view in the order of meters.

The best fit for the technology is where there is inherent motion of the object, for instance on a conveyor in a production environment. If no inherent motion is available the camera or laser must be scanned over the scene.

The main limitations of the technology are that triangulation always gives occlusion, and that laser speckles and laser line thickness limits the precision for very small field-of-views.

4. 3D technology overview

Many different 3D imaging techniques are used in a large variety of applications. Here we give a short summary of the main techniques and discuss their suitability for different applications. In this discussion only triangulation and time-of-flight based systems will be discussed. Other 3D methods such as interferometry and shape from shading are less common in industrial applications.

4.1. Stereo and fixed-pattern triangulation

Stereo imaging is a triangulation technique which uses the correlation between two or more camera images to calculate distance. A similar technology, found for instance in the Microsoft Kinect, is using a fixed pseudo random pattern illumination that has been taught in during calibration as one “camera” and a single real camera.

The key element of the methods is to correlate a patch in an image with number of patches in another image (stereo) or with a set of calibrated illumination pattern patches (Kinect). The best match defines the second angle of the triangle; the reference defines the first angle, and with a known baseline the triangulation equations can be solved, see Figure 11. An overview of stereo algorithms can be found in [8], and the Middlebury Stereo Vision Page [9] continues to benchmark stereo algorithms on their test data sets.

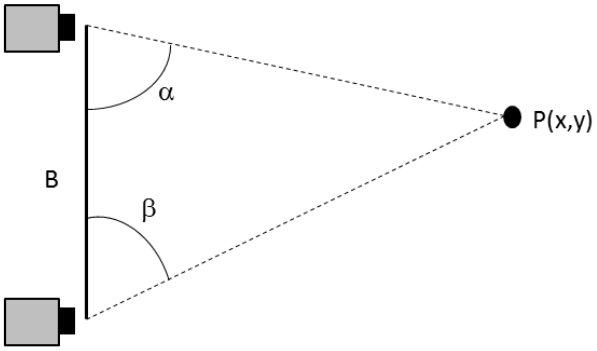

Figure 11. Illustration of the triangulation basics in stereo imaging. The setup defines the Baseline B, a pixel in the reference camera the angle α. the matching algorithm gives β, and the position P(x,y) can then be calculated.

The main benefit of this technology is that it gives true snapshot 3D data and as proven by the Kinect can be manufactured in an affordable and small package. The main drawback of the method is that a patch of pixels are needed for the matching, so that the end resolution image will not have independent measurements in each sensor pixel, and that the depth resolution is somewhat limited. Also, if there is no structure in the scene and no structure added by an illumination the results are very poor. A key factor to the robustness of the Kinect is the pseudo random pattern illuminating the scene with IR light and a very narrow band optical filter in the receiver to reduce the influence from the ambient light.

4.2. Spatially coded light

Spatially coded light systems illuminate the scene with multiple patterns and process a set of images to acquire depth information. Patterns are typically binary Gray-coded, giving 2^M triangulation direction for M patterns, or using a sinusoidal modulation. With a sinusoidal modulation phase shifted at least to three distinct angles, e.g. 0,120,240 degrees it is possible to calculate the phase, and thereby triangulation direction, seen by each pixel. If the modulation frequency is high the precision in the angle measurement is high, but also ambiguous due to multiple possible rays separated by 360 degree phase shifts. To handle this phase unwrapping problem multiple modulation frequencies or a combination of sinusoidal and binary patterns are employed [10]. The rapid development of DLP projection devices and high-power LED illuminations have made these systems faster, more compact and needing less maintenance the last years [11][12][13].

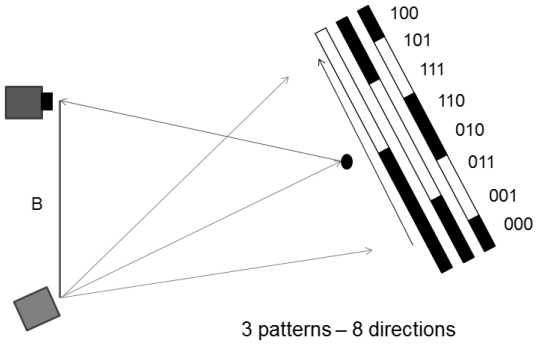

Figure 12. An illustration of spatially coded structured light illumination, where 3 Gray-coded binary patterns give 8 distinct triangulation directions.

The main benefit of the method is that it can give dense and very accurate 3D data, with an independent measure from each pixel in the sensor. The main drawback is that the scene cannot have any motion during the acquisition of the image sequence, and that the modulation of the pattern must be possible to measure. There is work combining stereo with phase coded structured light to overcome the problem of object motion, see for instance in [14].

4.3. TOF cameras

The time-of-flight (TOF) principle is simple; it measures the time for an electromagnetic pulse to travel from the transmitter to the object and back. The main difficulty using this is the high speed of the light traveling through space, so that very short times must be measured accurately.

Instead of measuring the direct travel time it is possible to use a continuous modulated wave (CW), and measure the phase difference between the transmitted and received signal. A third method uses very precise shutter timing, so that only a well-defined portion of the signal is seen. The relation between the signal seen at e.g. the "early" part of the receiving time and the complete signal can be used to compute the distance. An overview of TOF image sensors is found in [30].

Typically cameras based on time-of-flight have been based on the CW principle. A main drawback for the CW method is that it gives ambiguities in a similar way as high modulation frequency does in spatially coded light, and that the array resolutions so far are small, no more than QVGA. For high-precision measurements the depth resolution is not good enough either, and it is difficult to reach precision below a few centimeters.

4.4. Comparisons

The suitability for each method in solving an application depends on the application. Some generic observations were given above for each technology.

A test of different 3D sensors for use in Robot applications is found in [31]. This overview covers laser triangulation, fixed pattern triangulation, spatially coded light and TOF cameras. The laser triangulation based Ranger and Scanning Ruler systems from SICK both get good marks for precision tasks where ambient light issues might be present. The spatially coded light system performed well when ambient was not an issue.

If low point density is acceptable the fixed-pattern triangulation system from Scape technology [32] was found to deliver robust data for very varying surface conditions.

5. Application examples

In many industrial applications the objects are transported along a conveyor. This motion makes a system measuring cross sections, such as sheet-of-light triangulation, very well suited for in-line measurements. This can be for instance shape and volume measurements in food processing, inspection of packaged goods and inspection of electronic components.

In applications where there is no motion the laser triangulation is typically not as easily adapted. In these motion of the camera or laser has to be added.

Below we give details of one application in each of these cases where our sheet-of-light triangulation has been used successfully.

5.1. Board scanning

One of the first applications for the MAPP sensor technology was in Wood inspection [16]. Here the ability to combine range imaging with other measurements, Multiscan, made the sensor outstanding [26][27]. A typical sensor and illumination setup for board inspection in a Multiscan configuration is illustrated in Figure 13.

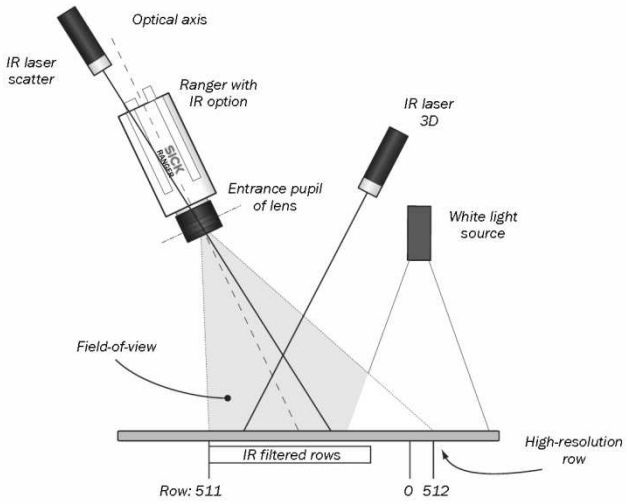

Figure 13. Typical multisense system combining 3D, laser scatter and grey or color imaging. Here an optional IR-pass filter covering a region on the sensor is shown. This reduces cross talk between white and laser illuminated regions.

In board quality inspection both geometrical and constructional defects are important, and therefore the ability to use laser scattering to see knots and different kinds of rot in addition to the range finding for dimensional inspection has proven important. When the M12 sensor was developed requirements from customers

in the wood inspection field was important and helped to define the new features of this sensor. For boards thin longitudinal cracks along the wood fibers is another important feature to detect, and the inclusion of a part of the array with double longitudinal pixel density helps this detection [28].

For the high resolution part of the sensor color filters were added in 2010 and this helps our customers further reduce system complexity by in effect incorporating a 3K wide color line scan sensor in the multi scan 3D camera.

A typical board scanning system contains 1 camera system for each side of the board, giving a 4-camera system. A depiction of a system implemented by the Wood scanning company Luxscan is seen in Figure 14 and Figure 15.

Figure 14. A board scanner from Weinig/Luxscan with 4 Ranger E cameras.

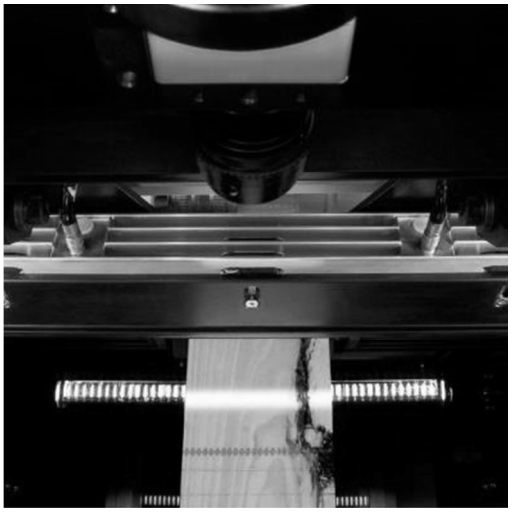

Figure 15. A look inside a board inspection system with the camera in the top of the image and the target with 4 different illuminations (white, 2 laser lines, 1 dotted laser line) on the board.

5.2. Robot Bin picking

Robot bin picking is a very demanding vision application. The goal is to allow a robot to pick parts that are arranged in a more or less random order in a bin. The robot can after picking up a part unload it in a predefined position and orientation, or directly manipulate the part. For bin picking applications SICK sells a system called PLB, Part Localization in Bins seen in Figure 16.

In contrast to the wood inspection application there is no inherent movement of the object, so the imaging system needs to image a complete static volume. For this purpose a laser triangulation system called Scanning Ruler using a rotating mirror to scan over the scene has been designed using the M12 sensor. The Scanning Ruler can image a volume of 800x1200x1000 mm with a typical resolution of 2 mm.

The PLB system also contains the necessary software components that are needed to give the robot information about where an object can be picked. The starting point of the localization of a part is learning the shape of the parts to pick. For this purpose a CAD model of the part is used. The system must also know how the piece can be picked up by the robot gripper. Given this information and an image from the Scanning Ruler the matching software can identify picking candidates. For the final selection of which part to pick up the system must also calculate how the robot arm can move to and from the picking position without colliding with other parts or the bin. To be able to use the system it is also important that the camera and robot coordinate systems are aligned, and this is made using a special calibration target and procedure.

The first PLB bin-picking system installations were made 2012.

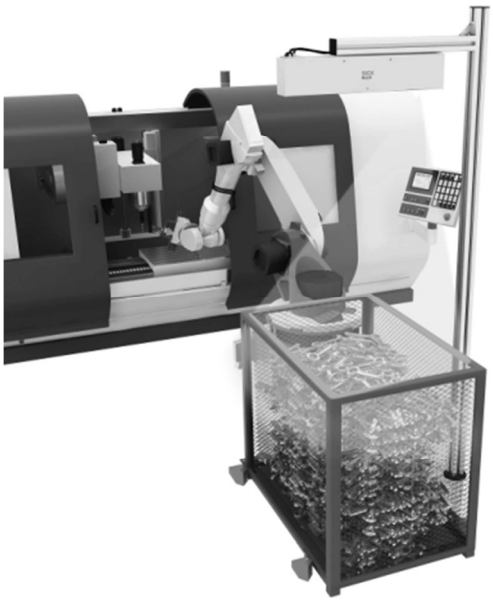

Figure 16. An illustration of a PLB bin picking system using the Scanning Ruler. 3D image data from the Scanning Ruler is used to control where the robot picks up an object.

6. Conclusions

We have shown how the general development in CMOS imaging has been used to implement a powerful family of sensors with on-board image processing and AD conversion. The high level of integration allows high performing, compact and power-efficient systems.

The sensor has proven to be very useful in 3D imaging using sheet-of-light triangulation.

We gave an overview of other state-of-the art 3D imaging technologies and their respective strength and weaknesses.

For typical industrial applications where objects are moved along a conveyor the sheet-of-light technology is the best fit, but we also showed an example where the technology is used to image static objects.

References

[1] Mattias Johannesson SIMD Architectures for Range and Radar Imaging, *Linköping Studies in Science and Technology, Dissertations No 399*, 1995.

[2] Mattias Johannesson, Anders Åström, Per-Erik Danielsson An Image Sensor for Sheet-of-Light Range Imaging, *Proc MVA '92* pp 43-46, 1992.

[3] Mattias Johannesson Fast, Programmable, sheet-of-light range finder using MAPP2200, *SPIE Vol 2273* , pp 25-34,1994.

[4] Mattias Johannesson, Sheet-of-light Range Imaging, *Linköping Studies in Science and Technology, Thesis No 404*, 1993.

[5] M Rioux, Laser Range Finder based on Synchronized scanners *Robot Sensors Vol 1 Vision*, e. A Pugh, Springer Verlag 1986.

[6] Araki K, et. al, A range finder with PSD's, *Proc MVA '90*, 1990.

[7] Verbeek P.W. et.al. Video-speed Triangulation Range Imaging, *NATO ASI Series, Vol F 63,* pp 181-186, Springer Verlag, 1990

[8] Scharstein D, Szeliski R, A taxonomy and Evaluation of Dense Two-Frame Stereo Correspondence Algorithms, *IJCV 2002*.

[9] http://vision.middlebury.edu/stereo/

[10] Huntley J.M., Saldner H.O. Shape Measurement by temporal phase unwrapping: comparison of unwrapping algorithms*, Measurement Science and Technology 8*, pp 986-992, 1997.

[11] Frankowski G., Chen M., Huth T., Real-time 3D Shape Measurement with Digital Stripe Projection by Texas Instruments Micromirror devices DMD, *SPIE Vol 3958 (2000) pp 90-106,* 2000

[12] Frankowski G., Hainich R., DLP-Based 3D-Metrology by Structured Light of Projected Fringe Technology for Life Sciences and Industrial Metrology., *proc of SPIE Photonics West* 2009.

[13] Zhang S., High-Resolution Real-time 3-D Shape Measurement, *Dissertation Stony Brook University,* 2005.

[14] Weise T., Leibe B., Van Gool L., Fast 3D Scanning with Automatic Motion Compensation, *IEEE Conference on Pattern Recognition (CVPR'07),* Minneapolis, 2007.

[15] Alder K, The Measure of All things – The seven year Oddesey and Hidden Error that Transformed the World, *ISBN 0-7432-1675-X*, 2002.

[16] Åstrand E, Automatic Inspection of Sawn Wood *Linköping Studies in Science and Technology, Dissertations No 424*, 1996.

[17] Forchheimer R, Ödmark A, A Single chip linear array processor, *SPIE Vol 397*, 1983.

[18] Forchheimer R, Ingelhag P, Jansson C, MAPP2200, a second generation smart sensor SPIE Vol 1659, 1992.

[19] Åström A, Forchheimer R, MAPP2200 Smart Vision Sensor. Programmability and Adaptivity, *Proc MVA '92* pp 17-20, 1992.

[20] Åström A, Smart image Sensors, *Linköping Studies in Science and Technology, Dissertations No 319*, 1993.

[21] Forchheimer R, Åström A, Near-sensor image processing: a new paradigm, *IEEE Transactions on Image Processing, Vol 3*, Issue 6, 1994.

[22] Lindgren L, Melander M, Johansson R, Möller B, A Multiresolution 100-GOPS 4-Gpixel/s Programmable Smart Vision Sensor for Multisense Imaging, *IEEE Journal of Solid-state circuits*, Vol 40, No 6, June 2005.

[23] Eric R. Fossum Active Pixel Sensors: Are CCD's Dinosaurs?, *SPIE Vol 1900*, 1993.

[24] Eric R. Fossum CMOS Image Sensors: Electronic Camera On A Chip, *IEDM* 1995.

[25] Forchheimer R, Ödmark A, Device for an array of photo diodes arranged in a matrix. *US Patent 4.684.991*, Applied 1984.

[26] Åstrand E, Åström A, Arrangement and method for the detection of defects in timber, *SE Patent 501.650*, Applied 1994.

[27] Åstrand E, Åström A, Method and arrangement in a measuring system, *EP patent 1.432.961*, applied 2001.

[28] Johannesson M, Murhed A, Arrangement in a measuring system, *SE Patent 523.681*, applied 2002.

[29] Johannesson M, Turbell H, Holm P, Measurement of light scatter, *US Patent 8.213.025*, applied 2007.

[30] Amud-ud-Din, Halin I.A., Shafie S.B., A review on solid state time of flight TOF range image sensors. *Proc of IEEE Student Conf. on Research and Development,* pp 246-249, 2009.

[31] Møller B., Balslev I., Krűger N., An automatic Evaluation Procedure for 3D Scanners in Robotics Applications, *IEE SensorsJournal Vol 13, Issue 2*, pp 870-878, Feb 2013.

[32] Blake A., Three-Dimensional Vision System, *PCT application WO 93/03579,* 1993.